ACS APPLIED NANO MATERIALS

www.acsanm.org Article

Effect of a Mixed Peptide Ligand Layer on Au Nanoparticles for Optical Control of Catalysis

Maichong Xie, Joseph M. Slocik, Nancy Kelley-Loughnane, and Marc R. Knecht*

Cite This: ACS Appl. Nano Mater. 2022, 5, 9379−9388 Read Online

ACCESS | Metrics & More | Article Recommendations | Supporting Information

ABSTRACT: Inorganic colloidal nanoparticles are known for their efficient catalytic reactivities due to their enhanced surface-to-volume ratio. As an alternative to conventional synthetic methods, bioinspired approaches can sustainably generate stable colloidal nanoparticles where their reactivity can be tuned by the biomolecular overlayer structure. Recent studies have shown that incorporation of light-activated photoswitches into material-binding peptides could be used to optically and reversibly switch the biomolecular overlayer structure on Au nanoparticle surfaces, which has significant ramifications on the material catalytic reactivity. In this contribution, we demonstrate that the optical photoswitching capability and catalytic reactivity in these materials are highly dependent upon the composition of the biomolecular overlayer. For this, mixed monolayer-capped Au nanoparticles were prepared where the ratio of the parent material-binding peptide and the peptide with photoswitch included were varied. Key trends related to the photoswitching capability of the peptides and their overall reactivity were identified, where slower reactivity was noted for materials prepared using only the photoswitchable peptide. Taken together, these results demonstrate that the composition of the overlayer structure on Au nanoparticles is highly important in tuning the overall optical, photoswitching, and catalytic properties of these materials and can be used to refine the properties of the structure for their intended application.

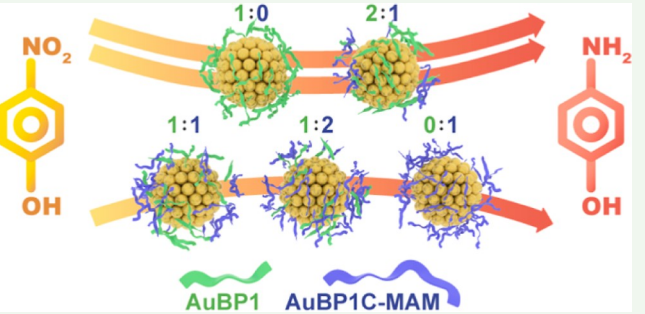

KEYWORDS: *nanoparticles, peptides, photoswitching, catalysis, response*

INTRODUCTION

Inorganic nanoparticles (NPs) have provided new avenues for catalytic activation based upon their enhanced surface-to-volume ratio that affords significant exposure of the catalytic materials.[1−3] To maintain their colloidal stability, the NPs must be passivated on the surface with some type of ligand that prevents uncontrolled aggregation of the materials to bulk precipitates.[4−7] These ligands are necessary to prevent aggregation; however, they also can diminish the NP reactivity by blocking catalytic active sites. While there are negative aspects to the surface-bound ligands, they also provide opportunities to incorporate additional functionality or handles to manipulate the properties of the reactive NPs or to engender the materials with secondary capabilities.[8−11]

Bioinspired approaches for NP synthesis are attracting a lot of interest for several reasons including facile synthetic approaches that are sustainable and the variety of functionalities that can be achieved from the NPs prepared through these methods.[12,13] In particular, material-binding peptides offer the ability to bind target materials specifically via noncovalent interactions that rival the strength of traditional organic ligands that bind covalently. To this end, the peptides bind through weak noncovalent interactions of the residues with the inorganic material that collectively lead to a strong overall affinity.[14−17] In addition, a wide set of peptides are known, as identified through biocombinatorial selection methods, with affinity for a variety of inorganic compositions, including noble metals, metal oxides, metal sulfides, and so forth.[12,13,18,19]

Peptide-derived Au NPs have been studied in depth, including identification of numerous sequences with affinity for this noble metal with the capability of tailoring the NPs' morphology and reactivity.[20−24] One peptide in particular isolated by Sarikaya and colleagues, AuBP1 (WAGAKRLVLRRE), has been extensively studied.[25−27] As previously demonstrated, the sequence has a high free energy of binding value (ΔG) of -40.7 ± 2.1 kJ/mol to Au,[28] where it binds to Au via a series of noncovalent interactions of the residues with the metallic surface. Remarkably, this binding affinity is highly sensitive to changes to the sequence; point mutations to the Trp-1, Arg-6, and Arg-11 anchor residues can

Received: April 18, 2022
Accepted: June 10, 2022
Published: June 24, 2022

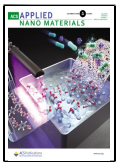

https://doi.org/10.1021/acsanm.2c01674
ACS Appl. Nano Mater. 2022, 5, 9379−9388

have significant implications on the observed binding affinity to Au.[28] Using the parent peptide, Au NPs of 4.2 ± 1.1 nm in diameter can be prepared,[26] which are stabilized in colloidal suspension in water via peptide/Au surface binding, leading to the formation of a biological overlayer structure.

Recent studies have demonstrated that chemical modification of the AuBP1 peptide can be exploited to make it responsive to optical irradiation; incorporation of an azobenzene-based photoswitch (termed MAM) into the peptide can be achieved, where this molecule can readily be switched between the cis and trans conformations via light.[29−31] When the peptide/MAM complex is used to stabilize Au NPs, the photoswitch can again isomerize; however, this isomerization event leads to dramatic changes in the biomolecular overlayer morphology on the material surface.[30−32] To this end, changes in the degree of surface contact of the individual residues of the biomolecule with the Au surface have been observed as a function of the MAM isomerization state. For instance, the Val-8 residue for the AuBP1C-MAM in the trans configuration has been observed to be in contact with the Au surface 60−79% of the time; however, for the same biomolecule in the cis conformation, the residue is in contact with Au only 20−39% of the time.[31] Similar changes have been observed in different residues of the biomolecule as a function of the MAM isomerization state, thus demonstrating notable changes in the overlayer structure. This change in ligand layer morphology can subsequently be exploited to modulate the catalytic properties of the Au NP, which was demonstrated for the reduction of 4-nitrophenol to 4-aminophenol. For instance, when the MAM unit was incorporated at the C-terminus of the peptide (termed AuBP1C-MAM), greater reactivity was noted for the NPs with the peptides in the trans conformation over the cis.[30] Additional research has demonstrated that the system is sensitive to not only the conformation of the photoswitch but also the peptide sequence used, the position of the photoswitch within the biomolecule, and the composition of the metallic NP.[29,33,34] To date, however, these NPs have only been studied with homogeneous peptide monolayers where all of the adsorbed biomolecules contain the integrated photoswitch. Monolayer morphologies were confirmed for both AuBP1 and AuBP1C-MAM sequences based upon their lack of dissipation energy during the quartz crystal microbalance analysis.[22,31] While these systems demonstrated interesting reactive properties, changes in their optical response may be achieved when mixed monolayers (e.g., both peptides with and without the photoswitch) are passivated at the NP surface.

Herein, the effect of the ligand layer peptide composition on Au NPs for both synthesis and catalytic properties is explored where changes in the reactivity were observed based upon the peptide surface composition. To this end, a mixed monolayer of AuBP1 peptides with and without the photoswitch (AuBP1 and AuBP1C-MAM, respectively) was prepared on the NP surface where the AuBP1/AuBP1C-MAM ratio was varied from 1:0 to 0:1. By changing the amount of photoswitchable peptide adsorbed onto the Au NP, direct modulation of the photoswitching process was noted, which had ramifications on the catalytic properties of the materials. In this regard, photoswitch isomerization rates were roughly equivalent for the mixed monolayer Au NPs; however, a dramatic increase in the cis to trans isomerization rate for the Au NPs capped with just AuBP1C-MAM was noted. In addition, a linear increase in the half-life of the cis isomer of the peptide was observed as the fraction of photoswitch-containing peptides in the mixed monolayer increased. Interestingly, a direct trend of diminished reactivity was noted as the fraction of AuBP1C-MAM on the Au NP surface increased. Taken together, these results provide key criteria for the design of photoswitchable NP ligands and their overlayer structure on the materials to modulate global material properties that could potentially be remotely stimulated for on-demand capabilities.

EXPERIMENTAL SECTION

Materials. Azobenzene-4,4′-dicarbonyl dichloride and *N*-(2-aminoethyl)maleimide hydrochloride were purchased from Tokyo Chemical Industry (TCI) and stored in a glovebox under an Ar atmosphere. Dichloromethane was purchased from Macron Fine chemicals, while additional organic solvents [triethylamine (TEA), *N*,*N*-dimethyl-formamide (DMF), and acetonitrile] were ordered from EMD Millipore. Diethyl ether and hydrochloric acid (36.5%−38%) were acquired from BDH. $HAuCl_4$ was purchased from Alfa Aesar, while $NaBH_4$ (97%) was acquired from Beantown Chemical. AuBP1 and AuBP1C peptides were commercially sourced from GenScript Biotech Corporation and stored at −80 °C. All reagents were used as received without additional treatment, and all aqueous-based experiments were performed with Milli-Q water (18 mΩ cm).

MAM Synthesis. The maleimide−azobenzene−maleimide (MAM) photoswitch was produced following the published protocol with modifications.[31] Briefly, azobenzene-4,4′-dicarbonyl dichloride (Azo) (30.82 mg, 0.1 mmol) and *N*-(2-aminoethyl)maleimide hydrochloride (Mal) (62.0 mg, 0.35 mmol) were fully dissolved in separate solutions with 5 mL of CH_2Cl_2 and 0.5 mL of TEA. Once prepared, the Mal solution was slowly added dropwise to the Azo solution, which was performed in an ice bath under a continuous N_2 flow. The mixture was then stirred for 2 days at room temperature, after which the solvent was evaporated using a rotovap. The solid sample was then washed twice with 10 mL of 0.1 M HCl.

Coupling of MAM and Peptide. Coupling of the MAM group to the AuBP1C peptide to generate AuBP1C-MAM was accomplished using established methods.[29−31] For this, 0.028 and 0.018 mmols of the MAM and peptide, respectively, (MAM/peptide = 1.6:1) were codissolved in 5 mL of DMF. The reaction was then stirred overnight to ensure significant coupling. Once complete, the sample was washed twice with ether (15 mL), the supernatant was decanted, and the precipitate was dissolved with water, which was subsequently lyopholized. The dried sample was then purified by reverse-phase HPLC and confirmed via MALDI-TOF mass spectrometry.

Synthesis of Peptide-Stabilized Au NPs. Standard procedures were employed to generate the peptide-capped Au NPs;[30,31] however, the ratio of peptides with and without the photoswitch on the material surface was varied. For this, five different AuBP1/AuBP1C-MAM peptide ratios were selected: 1:0, 2:1, 1:1, 1:2, and 0:1. Identical procedures were employed to prepare the final inorganic nanostructures, where only the amount of each peptide in the system was varied. Note that the total peptide concentration (AuBP1 + AuBP1C-MAM) remained constant. Using the 1:1 sample as an example, 1 mL of aqueous 0.25 mM AuBP1 solution and 1 mL of aqueous 0.25 mM AuBP1C-MAM solution were mixed and diluted with 2.96 mL of water. To this peptide solution, 10 μL of 100 mM $HAuCl_4$ solution (prepared in water) was added. This solution was stirred for 15 min to allow for complexation between the peptides and metal ions. Once complete, 30 μL of 100 mM $NaBH_4$ was slowly added into the system with gentle shaking, leading to Au ion reduction and NP formation.

Material Characterization. All UV−vis analyses, including photoswitching kinetics, half-life experiments, and catalytic studies, were conducted using an Agilent 8453 spectrophotometer. High-resolution transmission electron microscopy (HR-TEM) samples were prepared by dropping 5 μL of the diluted NP solution onto a carbon-coated copper TEM grid, which was then inverted and dried in a desiccator for at least 2 h. The samples were then imaged using a Tecnai F30 (FEI) instrument operating at 300 kV. For each sample, analysis of >120 NPs was processed where the diameter was measured

https://doi.org/10.1021/acsanm.2c01674
ACS Appl. Nano Mater. 2022, 5, 9379−9388

Scheme 1. Synthesis of AuBP1C-MAM (Top) and the Mixed Monolayer Peptide-capped Au NPs (Bottom)

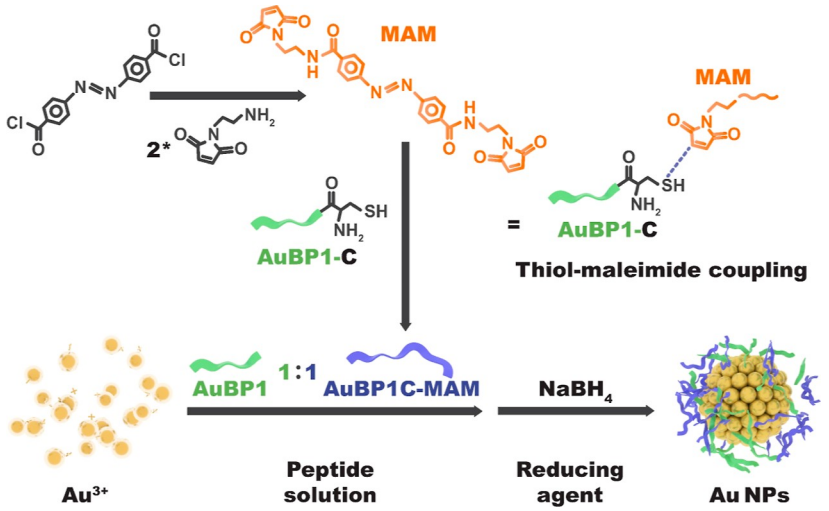

to identify the average particle size. X-ray photoelectron spectroscopy (XPS) data were collected on a Kratos AXIS Ultra spectrometer using a monochromated Al Kα source (1486.6 eV). The spectrometer was operated at 10 mA and 12 kV with an aperture spot size of approximately 300 × 700 μm. Samples were prepared by spotting 1 μL of the NP solution onto a clean silicon wafer and air dried. Survey scans were taken with an analyzer pass energy of 120 eV at 1 eV increments and a dwell time of 200 μs. High-resolution data of the Au 4f region were taken using a pass energy of 20 eV and a step size of 0.1 eV. Fourier transform infrared (FT-IR) spectroscopy was completed using a PerkinElmer Frontier spectrometer. For this analysis, the peptide-capped Au NPs were lyophilized to achieve a solid sample. Finally, dynamic light scattering (DLS) and ζ potential analyses were conducted using a ZETASIZER Nano series Nano-ZS (Malvern). Fresh Au NP solutions were filtered with a 0.2 μm syringe filter prior to each analysis.

Photoswitching and Half-Life Analysis. Photoinduced switching of the azobenzene residue in the surface-adsorbed peptides was processed using previously published procedures.[30,31] UV−vis analysis was employed to verify the switching via monitoring of the peak intensity at 330 nm. Analysis of each sample prepared as a function of the AuBP1/AuBP1C-MAM ratio was completed to observe changes in the switching event based upon the peptide surface composition. Once photoswitching was confirmed, the half-life of the peptides with the MAM in the cis conformation was studied at room temperature. For both analyses, the sample was switched into the cis conformation via irradiation of the sample with a handheld UV lamp (UVP UVL-21 Compact UV lamp, 365 nm) for 30 min. Once the photostationary state was achieved, changes in the absorbance at 330 nm were monitored over ∼5.5 h. The data were subsequently fit via first-order kinetics, as previously demonstrated,[30] to calculate the half-life of the cis conformation.

Catalytic Reactivity Analysis. Reduction of 4-nitrophenol to 4-aminophenol was processed with different peptide-capped Au NPs using well-established methods.[26,35−37] For this reaction, 450 μL of the prepared Au NPs and 45 μL of aqueous 4 mM 4-nitrophenol were commixed and then diluted with 975 μL of water in a glass vial. This mixture was transferred to a 1 cm quartz cuvette and allowed to reach the desired reaction temperature for 15 min. The reaction was then triggered by adding 30 μL of freshly prepared 3 M $NaBH_4$ solution in water, which was monitored by UV−vis spectroscopy via changes in the 4-nitrophenol absorbance at 400 nm for 2.5 min. For each NP system, the reaction was performed separately with the AuBP1C-MAM peptides in both trans and cis conformations. The reactions were processed over a temperature range of 15−30 °C where each reaction was fit using pseudo-first-order kinetics to quantify changes in reactivity as a function of the peptide surface composition.

RESULTS AND DISCUSSION

Incorporation of the photoswitching MAM residue into the AuBP1C peptide was achieved via standard thiol/maleimide coupling (Scheme 1).[29−31] Note that the cysteine residue in the AuBP1C sequence was added to facilitate MAM coupling. Once confirmed via MALDI-TOF mass spectrometry, the sequence was used to prepare the peptide-capped Au NPs. To generate the particles with a mixture of parent AuBP1 and photoswitching AuBP1C-MAM on the surface, the peptides were added into the reaction at select AuBP1/AuBP1C-MAM ratios. From this, the Au^{3+} ions were reduced with $NaBH_4$, resulting in Au NP growth and eventual capping by the peptides in solution (Scheme 1). This process resulted in a highly stable colloidal suspension of materials, regardless of the AuBP1/AuBP1C-MAM ratio in the reaction. Note that only the C-terminal modified AuBP1C-MAM photoswitchable peptide was explored. Prior studies have demonstrated that incorporation of the MAM at the N-terminus of the peptide (MAM-CAuBP1) generated NPs that were potentially unstable at elevated temperatures.[30]

To monitor NP production using the mixture of peptides in the reaction, UV−vis analysis was initially employed. For all studies, the system was blanked against the solvent, water. Figure 1a specifically presents the spectra of the peptides in solution prior to Au^{3+} addition where the AuBP1/AuBP1C-MAM ratio was varied, resulting in changes to individual peak intensities that directly corresponded to the AuBP1C-MAM concentration in the reaction. When considering the spectrum of the system with an AuBP1/AuBP1C-MAM ratio of 0:1 (purple spectrum), two peaks at 330 and 450 nm were observed. These peaks arise from the $\pi \rightarrow \pi^*$ and $n \rightarrow \pi^*$ transitions of the azobenzene moiety, respectively.[38] As the AuBP1/AuBP1C-MAM ratio changed with increasing amounts of the parent AuBP1 in the system, these peak intensities decreased. This was most prominently observed for the 330 nm peak. Finally, for the system with just AuBP1 present, no peaks associated with the MAM unit were observed, as anticipated. It is important to note that for all of the peptide samples, a peak at ∼280 nm was evident, which arises from the aromatic residues of the biomolecules.[39]

Figure 1b presents the same systems as in Figure 1a but after addition of two equivalents (based upon the total peptide concentration) of Au^{3+}. As anticipated, negligible changes in

https://doi.org/10.1021/acsanm.2c01674
ACS Appl. Nano Mater. 2022, 5, 9379−9388

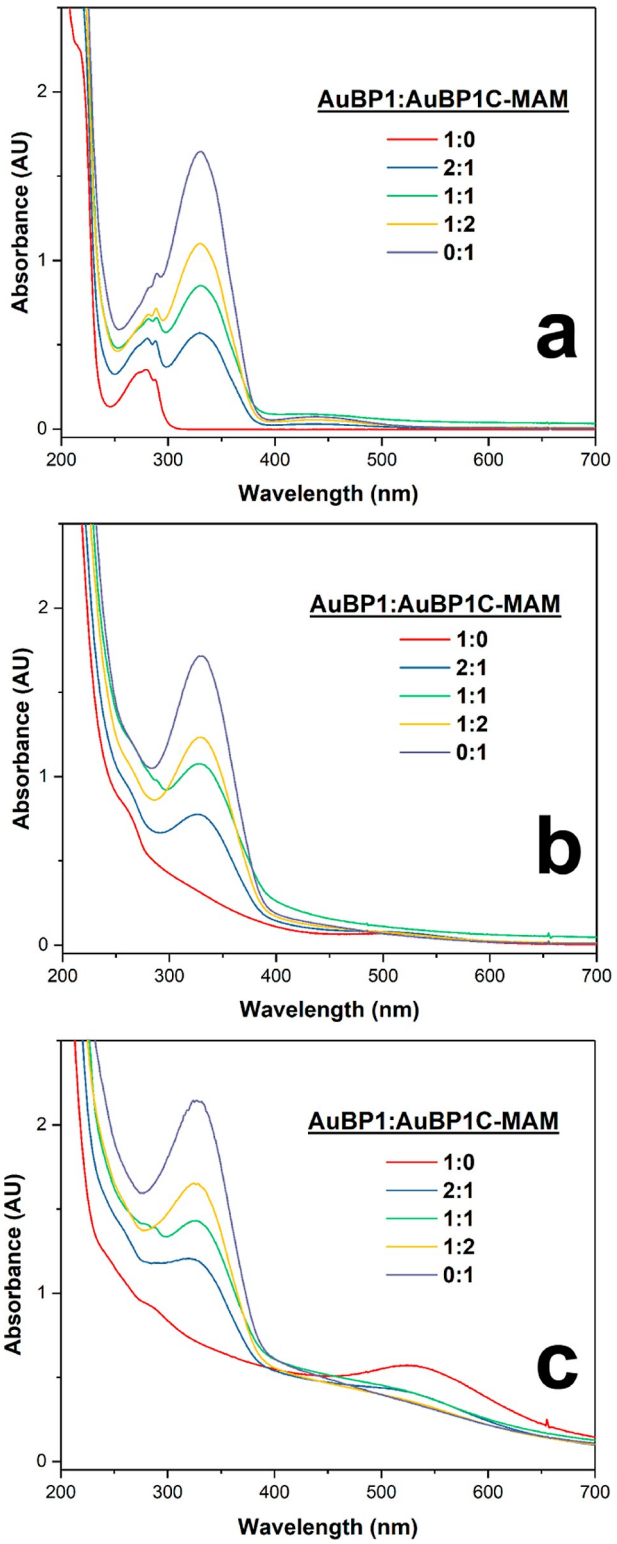

Figure 1. UV−vis analysis of Au NP synthesis at the indicated AuBP1:AuBP1C-MAM ratio at different stages: (a) peptides alone before Au^{3+} addition, (b) after addition of 2 equiv Au^{3+} to the reaction, and (c) after reduction with $NaBH_4$.

the spectra for each synthesis were observed. After reduction with $NaBH_4$, notable changes in the UV−vis spectra for the different NPs were noted, as shown in Figure 1c. For all of the materials prepared with AuBP1C-MAM present in the system, the absorbance of the azobenzene unit remained at 330 nm; however, the n → π^* transition was no longer observed at 450 nm. This lack of absorbance was due to the increase in absorbance toward lower wavelengths arising from the NPs generated in the system. Such a broad absorbance was consistent with the production of peptide-capped Au NPs.[26] It is important to note that the absorbance intensity at 330 nm was consistent with the amount of AuBP1C-MAM present in the sample, as anticipated. For some of the systems, a minor plasmon band was noted at 530 nm; however, a more significant plasmon absorbance was noted for the Au NPs capped with the parent peptide only (red spectrum). Such a plasmon band for this sample was anticipated, based upon prior studies, and may be reflective of differences in the size of the Au NPs prepared for the different systems.[40,41]

TEM analyses of the Au NPs capped with a mixed peptide layer are shown in Figure 2. For instance, the system prepared with a AuBP1/AuBP1C-MAM ratio of 2:1, presented in Figure 2a, demonstrated the production of spherical particles with an average size of 2.2 ± 0.8 nm. Similar Au NPs were observed for the other materials generated with AuBP1/AuBP1C-MAM ratios of 1:1 and 1:2 with average sizes of 1.9 ± 0.7 and 2.3 ± 0.8 nm, respectively (Figure 2b,c). In general, the materials were highly crystalline, as evidenced by the high-resolution images presented for each sample in the insert. Overall, such sizes were similar to that previously shown for the Au NPs capped with AuBP1C-MAM, which demonstrated a size of 2.7 ± 0.7 nm;[30] however, these structures were notably smaller than the Au NPs capped with the parent AuBP1 peptide without the photoswitch (4.2 ± 1.1 nm).[26] Such size results were consistent with the UV−vis observations for the AuBP1-capped Au NPs, where larger sized materials are known to generate a more vibrant plasmon.

Additional NP characterization was completed to more fully understand the material structure. XPS indicated that the systems were zerovalent metallic Au, which was fully reduced (Supporting Information, Figure S3). Low signal was observed from some samples during XPS analysis, which was likely due to low surface concentrations of the NPs. FT-IR analysis of the free peptides in solution and bound to the NP surface was also completed (Supporting Information, Figure S4). For all of the NPs, stretches associated with the peptide were noted in the sample; however, peak broadening and slight shifts were observed, which arise from adsorption of the biomolecules onto the material surface.[42] Finally, DLS and ζ potential analyses were conducted on the peptide-capped materials (Table S2 of the Supporting Information). DLS analysis indicated average NP diameters between 5.6 and 9.5 nm. Such sizes were reflective of the hydrodynamic diameter of the peptide-capped particles but were as anticipated based upon the TEM results. Finally, the ζ potential studies indicated that all of the particles were positively charged. Such a surface charge was the result of the positively charged peptide that possessed multiple amine-containing residues (e.g., lysine and arginine).

With confirmation of NP production using the mixed peptide systems, evaluation of the azobenzene photoswitching was completed (Figure 3). UV−vis analysis was employed to monitor the isomerization step, where the intensity of the π → π^* transition is highly sensitive to the isomerization state. To this end, trans to cis switching results in a diminished 330 nm peak intensity, while cis to trans switching leads to increased peak intensity.[38,43] To initiate the switching analysis, the peptide-capped NPs were irradiated for 30 min using UV light

https://doi.org/10.1021/acsanm.2c01674
ACS Appl. Nano Mater. 2022, 5, 9379−9388

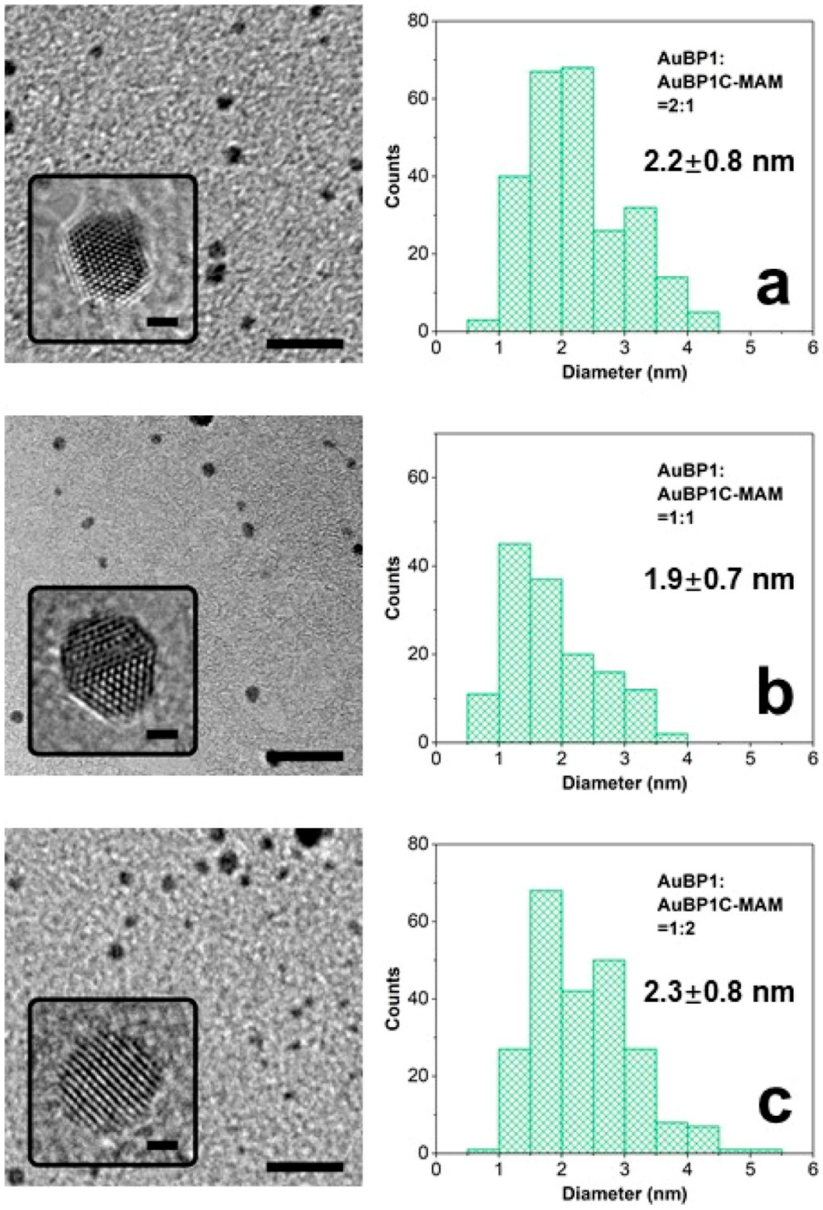

Figure 2. TEM analysis of the peptide-capped Au NPs at AuBP1/AuBP1C-MAM ratios of (a) 2:1, (b) 1:1, and (c) 1:2. The left panel presents the TEM image (scale bar = 10 nm), while the right panel shows the sizing analysis. A high-resolution image of a single particle is shown as an inset in the left panel (scale bar = 1 nm).

to induce trans to cis switching of the peptides adsorbed onto the Au surface. Figure 3a presents the analysis for the Au NPs prepared in the AuBP1/AuBP1C-MAM ratio of 2:1. In this case, trans to cis switching led to a decrease in the absorbance intensity (red to blue spectrum), as anticipated. When the sample was subsequently irradiated with visible light to drive cis to trans switching, the intensity of the 330 nm peak was restored, consistent with the expected isomerization. Identical effects were observed for all of the other systems that possessed photoswitchable peptides (Figure 3b–d), demonstrating that photoswitching was possible regardless of the AuBP1/AuBP1C-MAM ratio employed in the system.

To further probe the photoswitching event on the Au NP surface, the photoswitching rate constant (k_{iso}) and the half-life of the cis isomer were determined. As shown in Figure 4, the trans to cis and cis to trans switching rates were nearly identical for all three mixed monolayer materials, with a k_{iso} value of ~0.0014 s^{-1}. Remarkably, when the same study was completed with the Au NPs capped exclusively with photoswitchable AuBP1C-MAM, the rate of cis to trans switching was greater than trans to cis switching by more than 2-fold. That said, it is important to note that for this sample, the k_{iso} value for trans to cis switching was consistent with the rates observed for the mixed monolayer materials. Such results for the AuBP1C-MAM-capped NPs were consistent with previous studies,[31] but the differences for the mixed monolayer materials were somewhat surprising. This suggests that the inclusion of the parent AuBP1 peptides onto the NP surface alters cis to trans switching, potentially by facilitating the cis conformation of the MAM unit in the biomolecules adsorbed onto the material.

In addition to the rates of photoswitching, quantification of the half-life of the cis conformation of the MAM unit in the peptide was processed (Table 1). For this analysis, the half-life was measured for the peptides either free in solution at

https://doi.org/10.1021/acsanm.2c01674
ACS Appl. Nano Mater. 2022, 5, 9379–9388

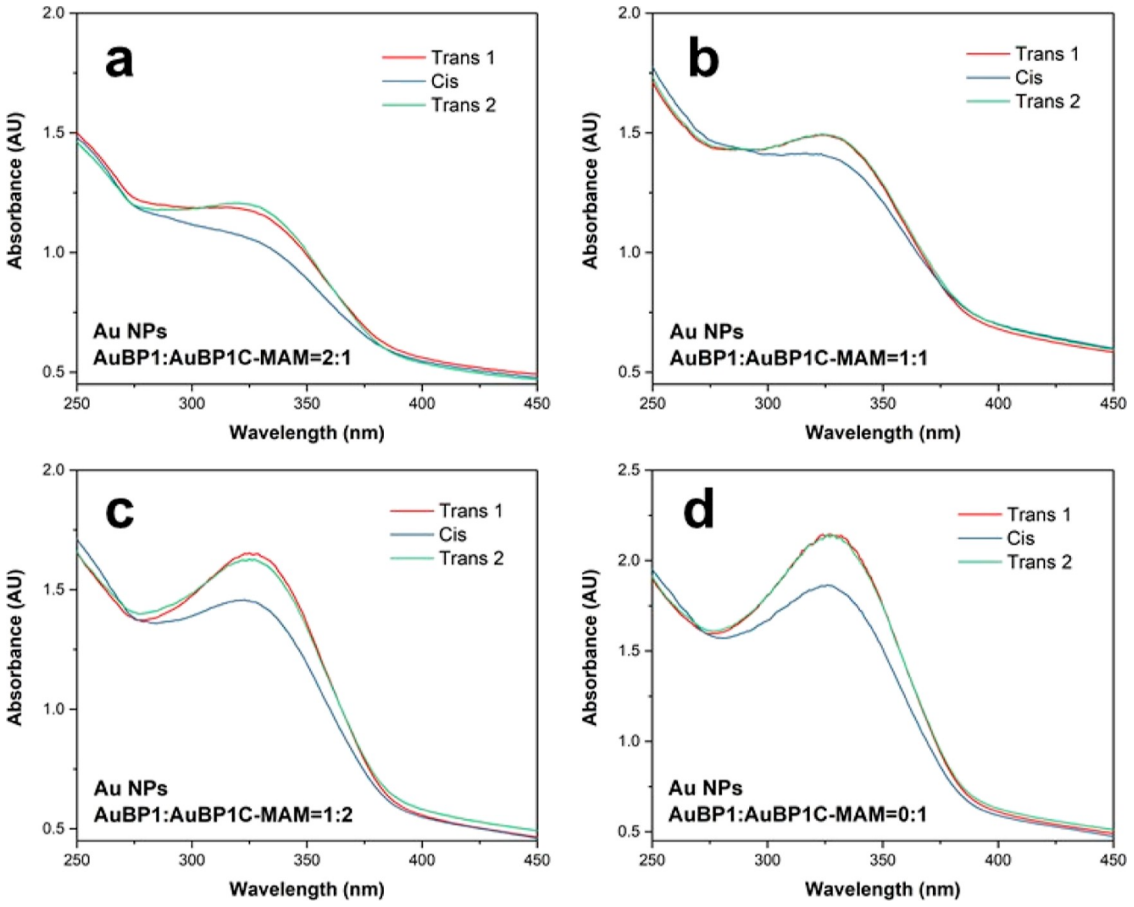

Figure 3. UV−vis spectra of MAM photoswitching for the Au NPs prepared in the AuBP1/AuBP1C-MAM ratio of (a) 2:1, (b) 1:1, (c) 1:2, and (d) 0:1.

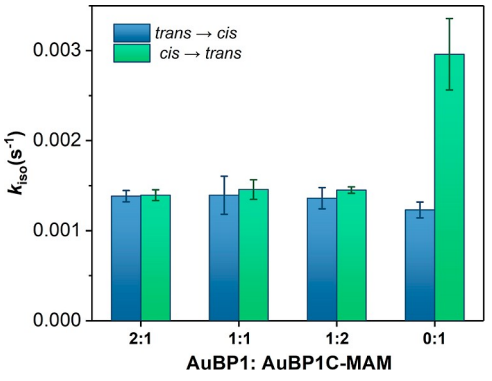

Figure 4. Photoswitching kinetics analysis for the peptide-capped Au NPs prepared at the indicated AuBP1/AuBP1C-MAM ratio.

Table 1. Half-Life Values for the Indicated Systems

mixed ratio	half-life	
AuBP1/AuBP1C-MAM	free peptides	capped on the NPs
2:1	5.3 ± 0.3	8.8 ± 1.5
1:1	5.1 ± 0.1	10.6 ± 3.3
1:2	5.7 ± 0.4	11.3 ± 8.0
0:1	7.1 ± 0.2	27.3 ± 9.4

appropriate AuBP1/AuBP1C-MAM ratios or bound to the NP surfaces. For both analyses, the half-life of the cis isomer generally increased as the amount of photoswitching AuBP1C-MAM peptide in the system increased. To this end, for the free peptides in solution, the half-lives ranged from 5.3 ± 0.3 h for a AuBP1/AuBP1C-MAM ratio of 2:1 to 7.1 ± 0.2 h for the system with just AuBP1C-MAM present. When the mixed monolayer-capped Au NPs were studied, the half-lives increased from 8.8 ± 1.5 to 27.3 ± 9.4 h over the range of AuBP1/AuBP1C-MAM ratios studied. It is noteworthy that a significant jump in the cis isomer half-life was observed between the materials with a AuBP1/AuBP1C-MAM ratio of 1:2 and the materials prepared with just AuBP1C-MAM. This further reinforces the effect of the AuBP1 parent in altering the cis to trans thermodynamic switching process, consistent with the observations of photoswitching rates (Figure 4).

From NP characterization, differences in the surface photoswitching were present based upon the AuBP1/AuBP1C-MAM ratio used for NP production, where these differences could directly affect the catalytic properties of the materials. To probe these catalytic property changes, the reduction of 4-nitrophenol to generate 4-aminophenol was processed. This is an ideal reaction for several factors. Most importantly, the reaction is processed directly on the exposed metallic surface, and thus the rate of catalytic turnover is directly related to the amount of available catalytic surface area on the NP.[44] Since the NP surface area, and thus available catalytic active sites, is anticipated to change based upon the trans versus cis conformation of the peptides, this makes the 4-nitrophenol reduction reaction an ideal choice.

For this reaction, the Au NP catalyst and 4-nitrophenol reactant were mixed and diluted with water. This mixture was

https://doi.org/10.1021/acsanm.2c01674
ACS Appl. Nano Mater. 2022, 5, 9379−9388

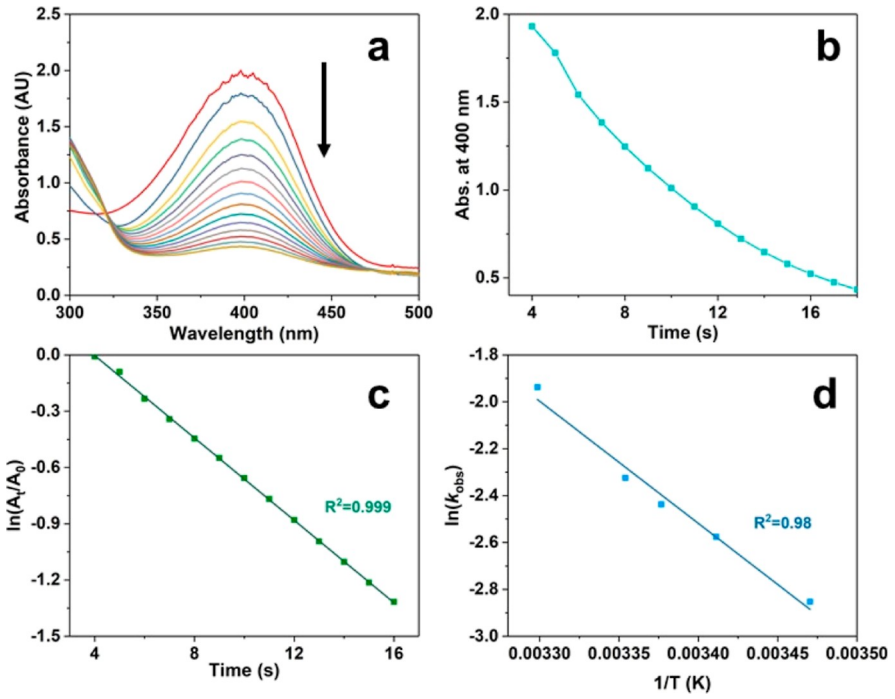

Figure 5. Analysis of 4-nitrophenol reduction reaction catalyzed by the peptide-capped Au NPs prepared in the AuBP1:AuBP1C-MAM ratio of 1:1 in the trans conformation. Part (a) presents the UV−vis analysis of the reaction as a function of time, while part (b) displays the change in absorbance at 400 nm over time. Part (c) shows the plot of $\ln(A_t/A_0)$ vs time from which reaction rate constants can be determined. Finally, part (d) presents an Arrhenius plot to extract E_a and A values.

allowed to equilibrate for 15 min to reach the reaction temperature, after which $NaBH_4$ was added to initiate the reaction. Once initiated, the reaction was monitored using UV−vis spectroscopy to observe the rate of 4-nitrophenol consumption via its absorbance at 400 nm (Figure 5a) where the intensity of the peak over time is shown in Figure 5b. Note that H_2 bubbles were generated in the reaction from the decomposition of $NaBH_4$ in H_2O, thus interfering with the observation of an isosbestic point for the reaction, as previously shown.[36] The same procedure was employed for both trans and cis conformations of the Au NPs; however, for the cis system, the NPs were irradiated for 30 min with UV light to ensure that the appropriate isomer was present on the material surface. It is important to note that the reaction was complete within 2.5 min, and thus the effect of thermally driven cis to trans switching that takes on the order of hours to complete is not anticipated to affect the catalytic process.

Once the reaction was processed, the first-order rate constants (k_{obs}) were extracted from the UV−vis data via standard approaches (Figure 5c). Note that since the $NaBH_4$ was in such a significant excess, the reaction was pseudo-first-order with respect to the 4-nitrophenol substrate. Figure 6a presents the analysis for the peptide-capped Au NPs with the photoswitch in the trans conformation as a function of reaction temperature. When considering the reaction processed at a temperature of 15 °C, a direct correlation between the AuBP1/AuBP1C-MAM ratio used in the system and the k_{obs} values was evident. To this end, for the AuBP1-capped Au NPs, a rate constant of $(7.6 \pm 0.6)\ 10^{-2}\ s^{-1}$ was achieved. For the Au NPs prepared with a minimal amount of AuBP1C-MAM in the monolayer (AuBP1/AuBP1C-MAM ratio 2:1), an identical k_{obs} value of $(7.6 \pm 0.1)\ 10^{-2}\ s^{-1}$ was also determined; however, the value then decreased as the amount of AuBP1C-MAM on the NP surface increased. To this end, for the AuBP1C-MAM-capped Au NPs, the smallest rate constant was observed at 15 °C with a value of $(5.1 \pm 0.4)\ 10^{-2}\ s^{-1}$. Similar effects were noted for the other trans-based materials regardless of the reaction temperature. As the reaction temperature increased from 15 to 30 °C, the k_{obs} values for each NP-driven reaction increased, as anticipated. For instance, for the Au NPs capped with peptides in the AuBP1/AuBP1C-MAM ratio of 2:1, the k_{obs} values ranged from $(7.6 \pm 0.1)\ 10^{-2}\ s^{-1}$ at 15 °C to $(16.8 \pm 0.1)\ 10^{-2}\ s^{-1}$ at 30 °C. Identical effects were observed for all of the samples with the peptides in the trans conformation, regardless of the AuBP1/AuBP1C-MAM ratio in the system.

When the reaction was processed with the Au NPs with the peptides in the cis conformation (Figure 6b), identical trends were calculated based upon the AuBP1/AuBP1C-MAM ratio and temperature; however, the k_{obs} values were lower as compared to the same system with the peptide in the trans conformation. Note that no data are presented for the AuBP1-capped Au NPs since these materials were not able to photoswitch. When comparing the reactivity for the Au NPs capped with peptides in the AuBP1/AuBP1C-MAM ratio of 2:1 at a temperature of 20 °C, a k_{obs} value of $(10.5 \pm 0.2)\ 10^{-2}\ s^{-1}$ was noted for the trans conformation that decreased to $(9.4 \pm 0.7)\ 10^{-2}\ s^{-1}$ for the NPs in the cis conformation. A direct comparison of each NP system at each temperature is presented in Figure S2 of the Supporting Information. Regardless of the MAM isomerization states, clear trends in the catalytic activity were observed, indicative of diminished k_{obs} values as the amount of AuBP1C-MAM in the system increased. This demonstrates that changes in the bio-overlayer structure were present on the materials as a function of the AuBP1/AuBP1C-MAM ratio used for NP synthesis. Attempts were made to experimentally measure the actual peptide ratio

https://doi.org/10.1021/acsanm.2c01674
ACS Appl. Nano Mater. 2022, 5, 9379−9388

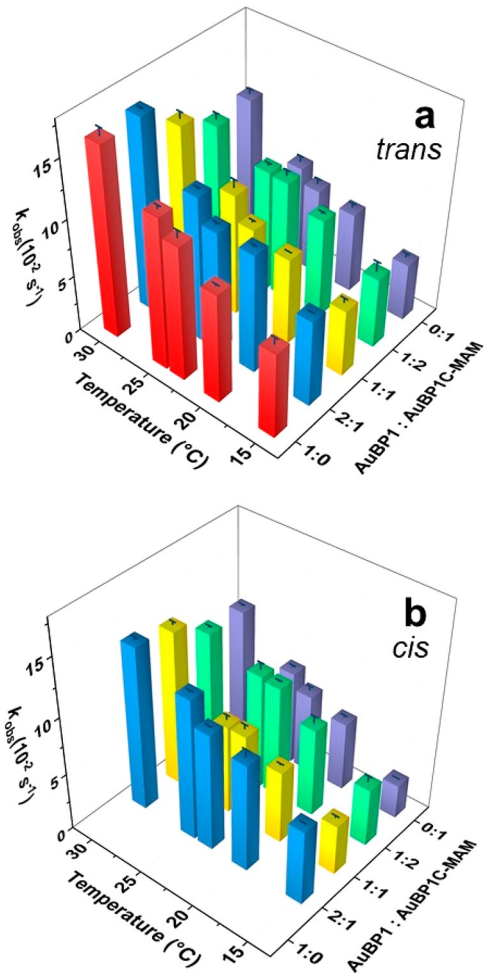

Figure 6. Rate constant (k_{obs}) comparison for the reduction of 4-nitrophenol at the indicated temperature using the peptide-capped Au NPs in the (a) trans and (b) cis conformations.

of the biomolecules adsorbed onto the sample; however, such studies were inconclusive due to material aggregation.

From the temperature-based catalytic analysis, extraction of activation energies (E_a) and frequency factors (A) can be achieved and compared (Figures 5d and 7). In general, for the NPs capped with a portion of the monolayer containing AuBP1C-MAM photoswitchable peptides, the NPs with the MAM conformation in the cis state presented higher E_a values over the same NPs in the trans conformation. This directly correlates with the observed k_{obs} value comparison, which demonstrated lower rate constants for the cis-based materials. In addition, the E_a values generally increased as the amount of AuBP1C-MAM increased in the monolayer. This is likely the basis for lower rate constants as the AuBP1/AuBP1C-MAM ratio increases. The outlier for this system is the NPs prepared in the AuBP1/AuBP1C-MAM ratio of 1:2, which had a lower E_a than anticipated. Interestingly, it also presents the lowest A value compared to the NPs prepared in the AuBP1/AuBP1C-MAM ratio of 1:1 and 0:1 (Figure 7b). The lower E_a value should result in a faster reaction as compared to the other NPs; however, the very low A value for this system suggests fewer collisions between the materials and the substrate that would result in catalytic turnover and product formation. This demonstrates that while trends were evident based upon the AuBP1/AuBP1C-MAM ratio used in the system, the observed catalytic rates are quite complex and dominated by a mixture of activation energy and frequency factors that work together to control the overall catalytic properties, as discussed for the 1:2 AuBP1/AuBP1C-MAM-capped Au NPs. Nevertheless, the reactions were shown to be directly affected by the conformation of the peptide on the NPs surface where enhanced reactivity for the peptides in the trans conformation was evident.

CONCLUSIONS

In summary, the effect of the composition of the peptide-capping monolayer on the surface of Au NPs was explored for remote optical control of the material catalytic properties. The results demonstrated clear trends associated with the ratio of peptide with and without the photoswitch incorporated (AuBP1/AuBP1C-MAM), which was used to prepare the materials, especially for their catalytic reactivity. In general, all of the samples were able to photoisomerize; however, the presence of the parent AuBP1 peptide was able to attenuate the rate of photoswitching. In addition, a trend of longer half-lives as the amount of AuBP1C-MAM in the system increased was noted. When considering the catalytic reactivity, changes in the reaction rate constants were noted in that the k_{obs} values decreased with more AuBP1C-MAM present on the NP surface. Furthermore, faster reactions for the peptide in the trans conformation over the cis were noted, regardless of the AuBP1/AuBP1C-MAM ratio employed. Taken together, these results highlight key design criteria to modulate the catalytic properties of optically responsive materials, which, in

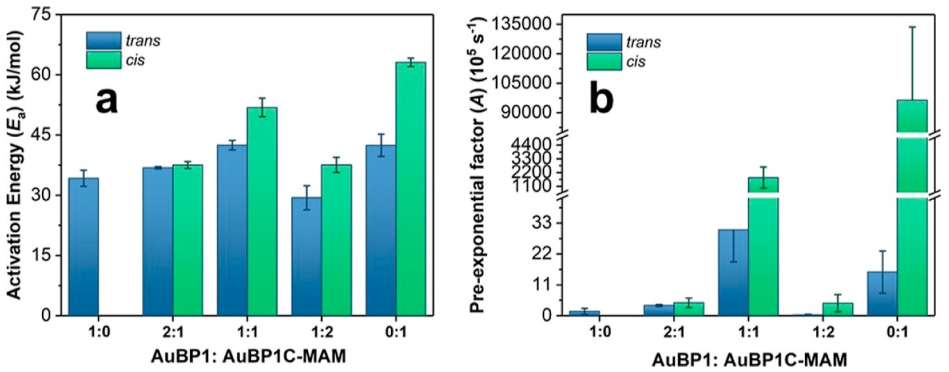

Figure 7. Comparison of the (a) activation energy (E_a) and (b) pre-exponential factors (A) for the reduction of 4-nitrophenol for the indicated peptide-capped Au NPs in either the trans or cis conformation.

https://doi.org/10.1021/acsanm.2c01674
ACS Appl. Nano Mater. 2022, 5, 9379−9388

combination with other key characteristics (peptide sequence, metal composition, etc.) could be used to finely tune the reactivity and responsivity of the NP system.

■ ASSOCIATED CONTENT

Supporting Information

The Supporting Information is available free of charge at https://pubs.acs.org/doi/10.1021/acsanm.2c01674.

Additional UV−vis, XPS, FT-IR, DLS, and ζ potential characterization data of NP synthesis and catalytic reactivity analysis (PDF)

■ AUTHOR INFORMATION

Corresponding Author

Marc R. Knecht − *Department of Chemistry, University of Miami, Coral Gables, Florida 33146, United States; Dr. J.T. Macdonald Foundation Biomedical Nanotechnology Institute, University of Miami, Miami, Florida 33136, United States;* orcid.org/0000-0002-7614-7258; Email: knecht@miami.edu

Authors

Maichong Xie − *Department of Chemistry, University of Miami, Coral Gables, Florida 33146, United States;* orcid.org/0000-0002-1654-952X

Joseph M. Slocik − *Materials and Manufacturing Directorate, Air Force Research Laboratory, Dayton, Ohio 45433, United States*

Nancy Kelley-Loughnane − *Materials and Manufacturing Directorate, Air Force Research Laboratory, Dayton, Ohio 45433, United States;* orcid.org/0000-0003-2974-644X

Complete contact information is available at: https://pubs.acs.org/10.1021/acsanm.2c01674

Author Contributions

This manuscript was written through the contributions of all of the authors. All authors approved the final version of the manuscript.

Notes

The authors declare no competing financial interest.

■ ACKNOWLEDGMENTS

This material is based upon work supported by the National Science Foundation under grant no. 1903649 (M.R.K.).

■ REFERENCES

(1) Auffan, M.; Rose, J.; Bottero, J.-Y.; Lowry, G. V.; Jolivet, J.-P.; Wiesner, M. R. Towards a definition of inorganic nanoparticles from an environmental, health and safety perspective. *Nat. Nanotechnol.* **2009**, *4*, 634−641.

(2) Goodman, E. D.; Zhou, C.; Cargnello, M. Design of organic/inorganic hybrid catalysts for energy and environmental applications. *ACS Cent. Sci.* **2020**, *6*, 1916−1937.

(3) Lohse, S. E.; Murphy, C. J. Applications of colloidal inorganic nanoparticles: from medicine to energy. *J. Am. Chem. Soc.* **2012**, *134*, 15607−15620.

(4) Villa, A.; Wang, D.; Su, D. S.; Prati, L. Gold sols as catalysts for glycerol oxidation: The role of stabilizer. *ChemCatChem* **2009**, *1*, 510−514.

(5) Wang, W.; Wei, Q.-Q.; Wang, J.; Wang, B.-C.; Zhang, S.-h.; Yuan, Z. Role of thiol-containing polyethylene glycol (thiol-PEG) in the modification process of gold nanoparticles (AuNPs): stabilizer or coagulant? *J. Colloid Interface Sci.* **2013**, *404*, 223−229.

(6) Zhang, G.-R.; Xu, B.-Q. Surprisingly strong effect of stabilizer on the properties of Au nanoparticles and Pt̂ Au nanostructures in electrocatalysis. *Nanoscale* **2010**, *2*, 2798−2804.

(7) Zhong, R.-Y.; Yan, X.-H.; Gao, Z.-K.; Zhang, R.-J.; Xu, B.-Q. Stabilizer substitution and its effect on the hydrogenation catalysis by Au nanoparticles from colloidal synthesis. *Catal. Sci. Technol.* **2013**, *3*, 3013−3019.

(8) Han, Y.; Li, J.; Zhang, X.; Xia, F.; Dai, Y. Reversible down-regulation and up-regulation of catalytic activity of poly (N-isopropylacrylamide)-anchored gold nanoparticles. *Nanotechnol* **2022**, *33*, 165601.

(9) Liu, R.; Zhang, X.; Xia, F.; Dai, Y. Azobenzene-based photoswitchable catalysts: State of the art and perspectives. *J. Catal.* **2022**, *409*, 33−40.

(10) Tan, X.; Xu, Y.; Lin, S.; Dai, G.; Zhang, X.; Xia, F.; Dai, Y. Peptide-anchored gold nanoparticles with bicatalytic sites for photo-switchable cascade catalysis. *J. Catal.* **2021**, *402*, 125−129.

(11) Zhang, X.; Lin, S.; Wang, Y.; Xia, F.; Dai, Y. Cofactor-free organic nanozyme with assembly-induced catalysis and light-regulated activity. *J. Chem. Eng.* **2021**, *426*, 130855.

(12) Walsh, T. R.; Knecht, M. R. Biointerface structural effects on the properties and applications of bioinspired peptide-based nanomaterials. *Chem. Rev.* **2017**, *117*, 12641−12704.

(13) Walsh, T. R.; Knecht, M. R. Biomolecular material recognition in two dimensions: peptide binding to graphene, h-BN, and MoS2 nanosheets as unique bioconjugates. *Bioconjugate Chem.* **2019**, *30*, 2727−2750.

(14) Palafox-Hernandez, J. P.; Lim, C.-K.; Tang, Z.; Drew, K. L. M.; Hughes, Z. E.; Li, Y.; Swihart, M. T.; Prasad, P. N.; Knecht, M. R.; Walsh, T. R. Optical actuation of inorganic/organic interfaces: comparing peptide-azobenzene ligand reconfiguration on gold and silver nanoparticles. *ACS Appl. Mater. Interfaces* **2016**, *8*, 1050−1060.

(15) Palafox-Hernandez, J. P.; Tang, Z.; Hughes, Z. E.; Li, Y.; Swihart, M. T.; Prasad, P. N.; Walsh, T. R.; Knecht, M. R. Comparative study of materials-binding peptide interactions with gold and silver surfaces and nanostructures: a thermodynamic basis for biological selectivity of inorganic materials. *Chem. Mater.* **2014**, *26*, 4960−4969.

(16) Tamerler, C.; Oren, E. E.; Duman, M.; Venkatasubramanian, E.; Sarikaya, M. Adsorption kinetics of an engineered gold binding peptide by surface plasmon resonance spectroscopy and a quartz crystal microbalance. *Langmuir* **2006**, *22*, 7712−7718.

(17) Sultan, A. M.; Westcott, Z. C.; Hughes, Z. E.; Palafox-Hernandez, J. P.; Giesa, T.; Puddu, V.; Buehler, M. J.; Perry, C. C.; Walsh, T. R. Aqueous peptide−TiO2 interfaces: Isoenergetic binding via either entropically or enthalpically driven mechanisms. *ACS Appl. Mater. Interfaces* **2016**, *8*, 18620−18630.

(18) Chen, C.-L.; Rosi, N. L. Peptide-based methods for the preparation of nanostructured inorganic materials. *Angew. Chem., Int. Ed.* **2010**, *49*, 1924−1942.

(19) Yu, X.; Wang, Z.; Su, Z.; Wei, G. Design, fabrication, and biomedical applications of bioinspired peptide−inorganic nanomaterial hybrids. *J. Mater. Chem. B* **2017**, *5*, 1130−1142.

(20) Brown, S.; Sarikaya, M.; Johnson, E. A genetic analysis of crystal growth. *J. Mol. Biol.* **2000**, *299*, 725−735.

(21) Lee, N.; Lee, D.-W.; Lee, S.-M. Gold nanoparticle-stabilized, tyrosine-rich peptide self-assemblies and their catalytic activities in the reduction of 4-nitrophenol. *Biomacromolecules* **2018**, *19*, 4534−4541.

(22) Tang, Z.; Palafox-Hernandez, J. P.; Law, W.-C.; Hughes, Z. E.; Swihart, M. T.; Prasad, P. N.; Knecht, M. R.; Walsh, T. R. Biomolecular recognition principles for bionanocombinatorics: an integrated approach to elucidate enthalpic and entropic factors. *ACS Nano* **2013**, *7*, 9632−9646.

(23) Lévy, R. Peptide-Capped Gold Nanoparticles: Towards Artificial Proteins. *ChemBioChem* **2006**, *7*, 1141−1145.

(24) Slocik, J. M.; Stone, M. O.; Naik, R. R. Synthesis of gold nanoparticles using multifunctional peptides. *Small* **2005**, *1*, 1048−1052.

(25) Hnilova, M.; Oren, E. E.; Seker, U. O. S.; Wilson, B. R.; Collino, S.; Evans, J. S.; Tamerler, C.; Sarikaya, M. Effect of molecular conformations on the adsorption behavior of gold-binding peptides. *Langmuir* **2008**, *24*, 12440−12445.
(26) Li, Y.; Tang, Z.; Prasad, P. N.; Knecht, M. R.; Swihart, M. T. Peptide-mediated synthesis of gold nanoparticles: effects of peptide sequence and nature of binding on physicochemical properties. *Nanoscale* **2014**, *6*, 3165−3172.
(27) Munro, C. J.; Hughes, Z. E.; Walsh, T. R.; Knecht, M. R. Peptide sequence effects control the single pot reduction, nucleation, and growth of Au nanoparticles. *J. Phys. Chem. C* **2016**, *120*, 18917−18924.
(28) Nguyen, M. A.; Hughes, Z. E.; Liu, Y.; Li, Y.; Swihart, M. T.; Knecht, M. R.; Walsh, T. R. Peptide-mediated growth and dispersion of Au nanoparticles in water via sequence engineering. *J. Phys. Chem. C* **2018**, *122*, 11532−11542.
(29) Lawrence, R. L.; Olagunju, M. O.; Liu, Y.; Mahalingam, K.; Slocik, J. M.; Naik, R. R.; Frenkel, A. I.; Knecht, M. R. Remote controlled optical manipulation of bimetallic nanoparticle catalysts using peptides. *Catal. Sci. Technol.* **2021**, *11*, 2386−2395.
(30) Lawrence, R. L.; Scola, B.; Li, Y.; Lim, C.-K.; Liu, Y.; Prasad, P. N.; Swihart, M. T.; Knecht, M. R. Remote optically controlled modulation of catalytic properties of nanoparticles through reconfiguration of the inorganic/organic interface. *ACS Nano* **2016**, *10*, 9470−9477.
(31) Tang, Z.; Lim, C.-K.; Palafox-Hernandez, J. P.; Drew, K. L. M.; Li, Y.; Swihart, M. T.; Prasad, P. N.; Walsh, T. R.; Knecht, M. R. Triggering nanoparticle surface ligand rearrangement via external stimuli: light-based actuation of biointerfaces. *Nanoscale* **2015**, *7*, 13638−13645.
(32) Olagunju, M. O.; Liu, Y.; Frenkel, A. I.; Knecht, M. R. Atomically Resolved Characterization of Optically Driven Ligand Reconfiguration on Nanoparticle Catalyst Surfaces. *ACS Appl. Mater. Interfaces* **2021**, *13*, 44302−44311.
(33) Lawrence, R. L.; Cendan, V. J.; Scola, B.; Liu, Y.; Lim, C.-K.; Prasad, P. N.; Swihart, M. T.; Knecht, M. R. Optical Control of Biomimetic Nanoparticle Catalysts Based upon the Metal Component. *J. Phys. Chem. C* **2018**, *122*, 28055−28064.
(34) Lawrence, R. L.; Hughes, Z. E.; Cendan, V. J.; Liu, Y.; Lim, C.-K.; Prasad, P. N.; Swihart, M. T.; Walsh, T. R.; Knecht, M. R. Optical control of nanoparticle catalysis influenced by photoswitch positioning in hybrid peptide capping ligands. *ACS Appl. Mater. Interfaces* **2018**, *10*, 33640−33651.
(35) Briggs, B. D.; Li, Y.; Swihart, M. T.; Knecht, M. R. Reductant and sequence effects on the morphology and catalytic activity of peptide-capped Au nanoparticles. *ACS Appl. Mater. Interfaces* **2015**, *7*, 8843−8851.
(36) Wunder, S.; Polzer, F.; Lu, Y.; Mei, Y.; Ballauff, M. Kinetic analysis of catalytic reduction of 4-nitrophenol by metallic nanoparticles immobilized in spherical polyelectrolyte brushes. *J. Phys. Chem. C* **2010**, *114*, 8814−8820.
(37) Baruah, B.; Gabriel, G. J.; Akbashev, M. J.; Booher, M. E. Facile synthesis of silver nanoparticles stabilized by cationic polynorbornenes and their catalytic activity in 4-nitrophenol reduction. *Langmuir* **2013**, *29*, 4225−4234.
(38) Bandara, H. M. D.; Burdette, S. C. Photoisomerization in different classes of azobenzene. *Chem. Soc. Rev.* **2012**, *41*, 1809−1825.
(39) Esfandiary, R.; Hunjan, J. S.; Lushington, G. H.; Joshi, S. B.; Middaugh, C. R. Temperature dependent 2nd derivative absorbance spectroscopy of aromatic amino acids as a probe of protein dynamics. *Protein Sci.* **2009**, *18*, 2603−2614.
(40) Hostetler, M. J.; Wingate, J. E.; Zhong, C.-J.; Harris, J. E.; Vachet, R. W.; Clark, M. R.; Londono, J. D.; Green, S. J.; Stokes, J. J.; Wignall, G. D.; Glish, G. L.; Porter, M. D.; Evans, N. D.; Murray, R. W. Alkanethiolate gold cluster molecules with core diameters from 1.5 to 5.2 nm: core and monolayer properties as a function of core size. *Langmuir* **1998**, *14*, 17−30.
(41) Munro, C. J.; Knecht, M. R. Solution Effects on Peptide-Mediated Reduction and Stabilization of Au Nanoparticles. *Langmuir* **2017**, *33*, 13757−13765.
(42) Luo, J.; Cheng, Y.; Gong, Z.-W.; Wu, K.; Zhou, Y.; Chen, H.-X.; Gauthier, M.; Cheng, Y.-Z.; Liang, J.; Zou, T. Self-assembled peptide functionalized gold nanopolyhedrons with excellent chiral optical properties. *Langmuir* **2019**, *36*, 600−608.
(43) Beharry, A. A.; Woolley, G. A. Azobenzene photoswitches for biomolecules. *Chem. Soc. Rev.* **2011**, *40*, 4422−4437.
(44) Wunder, S.; Lu, Y.; Albrecht, M.; Ballauff, M. Catalytic activity of faceted gold nanoparticles studied by a model reaction: evidence for substrate-induced surface restructuring. *ACS Catal.* **2011**, *1*, 908−916.

https://doi.org/10.1021/acsanm.2c01674
ACS Appl. Nano Mater. 2022, 5, 9379−9388